A Logarithmic Spiral Antenna for 0.4 to 3.8 GHz

This article reviews the design, simulation and measured performance of a broadband antenna

By Jesper Thaysen, Kaj B. Jakobsen and Jørgen Appel-Hansen
Technical University of Denmark

This article discusses a low-cost cavity backed coplanar-waveguide to coplanar-strip fed logarithmic uniplanar spiral antenna that covers a 9:1 bandwidth with a return loss better than 10 dB from 0.4 to 3.8 GHz. The IE3D computer program is used to predict the performance of the spiral antenna in terms of radiation pattern and input impedance. The obtained numerical results are in good agreement with the experimental data. The spiral antenna radiates from an active region that is a frequency-dependent part of the structure. The rotation of the radiation pattern as a function of frequency will also be discussed.

Frequency independent antennas

Frequency independent antennas are antennas whose radiation pattern, impedance and polarization remain virtually unchanged over a large bandwidth [1]. Their electrical dimensions, however, scale with frequency. Ideally, the electrical size of such antennas would remain constant over the entire electromagnetic spectrum. This ideal state requires that the logarithmic spiral antenna be infinite to fulfill the self-scaling and self-complementary conditions. For a certain range of parameters, the logarithmic spiral antenna can be truncated and still retain the properties of the infinite structures over a very wide band. The practical frequency independent structure is truncated, which limits the antenna's upper and lower frequency limits [2, 3].

A broadband antenna could find wide application in many systems. This article is a part of the ongoing research at the Technical University of Denmark in the area of stepped-frequency ground penetration radar (SF-GPR) to detect buried non-metallic Anti-Personnel mines (AP-mines) in a humanitarian mine detection system [4].

In coaxial structures, such as coax cables, the electrical wavelength is changed by a factor of

$$\frac{1}{\sqrt{\varepsilon_r}}$$

due to the dielectric constant of the isolator [5]. In antenna systems, dielectric loading can be used with the same advantageous properties, although the antenna is a radiating structure. The resonant frequency of a patch antenna could be reduced using a piece of dielectric material placed on top of the antenna [5]. It is also possible to reduce the size of the antenna at a given resonant frequency.

Both the permittivity and the thickness of the substrate influence the performance. The loss in the material will alter the performance as well, so material with low loss is preferable. Thick substrates with a low dielectric constant provide better efficiency and larger bandwidth at the expense of larger element size. The same results can be obtained using a thin structure that has a higher dielectric constant, which is a trade-off between efficiency and the physical size of a given structure.

Dielectric loading seems to offer good possibilities for reducing the physical size of an antenna. It is therefore a very important design technique to meet requirements for size and resonance frequency for antenna design. IE3D is used to determine the influence of dielectric loading on the spiral antenna for various permittivity values. A simple 1.5 turn spiral antenna is used to investigate the dielectric loading

effect and the radiation efficiency.

Composite materials offer good mechanical and electrical properties and are available with dielectric constants in the range of 2 to 20. The RT/Duroid is an example of a composite with well-documented electrical, mechanical and temperature stability, and is therefore a popular material in planar antenna design. The disadvantages of this type of material are the availability and the cost.

The substrate used for this article is the FR-4 substrate, which is commonly used for printed circuits. The FR-4 board is less expensive than commonly used microwave substrates, such as RT/Duroid. This feature, combined with the advantages of the uniplanar circuit, makes this configuration suitable as a low cost wideband antenna. Nevertheless, the loss is increasing as a function of frequency for the FR-4 substrate, and the dielectric performance of the FR-4 could change from one manufacture to another, and from batch to batch.

To aid the antenna design, the electromagnetic simulation program (IE3D) computer program developed by Zeland Software [6], was used to predict the performance of the spiral antenna in terms of the radiation pattern and the input impedance. The measured results of the constructed antenna are compared to the simulated results.

Selection of the antenna type

The larger the frequency range, the better the range resolution is when using frequency-domain or time-domain techniques. Thus, the use of a broadband antenna is essential for the signal and image processing in order to improve the detection of non-metallic AP-mines. Because of the signal processing, it is desirable to make the sidelobes as small as possible.

The operating frequency range of the antenna for the SF-GPR is from 0.4 to 3.8 GHz, which yields a bandwidth of 3.4 GHz corresponding to a radar range resolution of about 40 mm in the soil. The lowest operation frequency of 0.4 GHz is a compromise between the ground attenuation and the antenna size, whereas the feeding network sets the limit at the high frequencies.

Although a linearly polarized log-periodic antenna has a wide bandwidth and is an attractive candidate, circular polarization is preferred to linear polarization for several. If a linearly polarized antenna is used, the strength of the reflected wave from an object will depend on the azimuthal position of the antenna relative to the object. Further, if the orientation of the transmitting and receiving antennas is orthogonal, the mutual coupling between the two linearly polarized antennas will be reduced. As a result, the receiving antenna would barely detect the reflected wave from the object. Circular polarization, however, does not have such problems. For this reason, spiral antennas were selected [7].

Another advantage of circular polarization is that the reflected signal from the surface of the soil has the opposite sense of polarization as compared to the incident wave, because the ratio between the permittivity of soil and air is larger than 1. Thus, the antenna does not detect the reflected wave from the surface. However, the reflected wave from the AP-mine has the same sense of polarization as the incident wave because the permittivity ratio between mine and soil is less than 1. This means that the only detected signal is the one reflected from an object having a relative permittivity lower than soil, for example, the AP-mines.

Among the spiral antennas, the conical spiral antenna radiates unidirectionally [8]. This unidirectionality of radiation is required for radar applications. However, for a conical spiral antenna, different frequency waves are radiated from different active regions of the cone. This gives rise to a problem for the range measurement, because the distance to the object depends on the frequency. This problem is reduced with the logarithmic spiral antennas because their shape is not conical but planar. However, the planar antennas have a bidirectional radiation property [2, 3]. By placing an absorbing material in a cavity behind the spiral antenna, the antenna exhibits a unidirectional radiation pattern. The disadvantage is that only half of the input power is transformed into radiated power because of the presence of the absorber. A specially designed reflector may also be used.
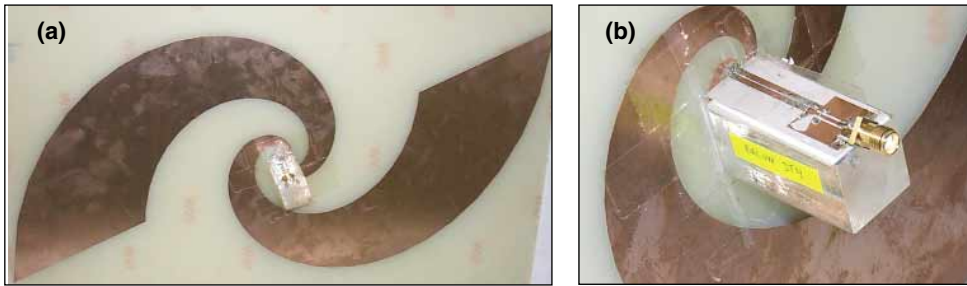
The principle of the spiral antenna

The logarithmic spiral antenna was designed using the equations $r_1 = r_0 e^{a\theta}$ and $r_2 = r_0 e^{a(\theta - \theta_0)}$, where r_1 and r_2 are the outer and inner radii of the spirals, respectively; r_0 and $r_0 e^{-a\theta_0}$ are the initial outer and inner radii; a is the growth rate; and θ is the angular position. To obtain the most frequency independent radiation pattern and the most constant input impedance, the dimensions are $r_0 = 2.1$ mm, $a = 0.5$ rad^{-1}, and $\theta_0 = 1.3$ rad = 75 degrees [2, 9].

With these design parameters, the width of the arms are the same as the spacing between the arms, and the structure is self-complementary, which gives the most frequency independent parameters [2].

Good radiation patterns can usually be obtained with as few as 1 to 1-1/2 turns of the spiral [2]. Thus, the spiral antenna illustrated in Figure 1 consists of two equal arms, each with a 1.5 turn. The ends of the two spiral arms are truncated to produce the smallest physical antenna for a given lower resonant frequency. Alternatively, the end of the spiral arms can be tapered, which will result in a more constant input impedance of the antenna. The spiral antenna is fabricated on a 220×430 mm FR-4 substrate, with a thickness of 1.5 mm and a relative dielectric constant (ε_r) of 4.4.

When the antenna arms are very short compared to one wavelength, the polarization is linear. As the fre-

▲ Figure 1. (a) Illustration of the spiral antenna placed on the FR-4 substrate. (b) Close up picture of the balun placed perpendicular to the plane of the antenna and soldered directly to the feed terminals on the spiral antenna.
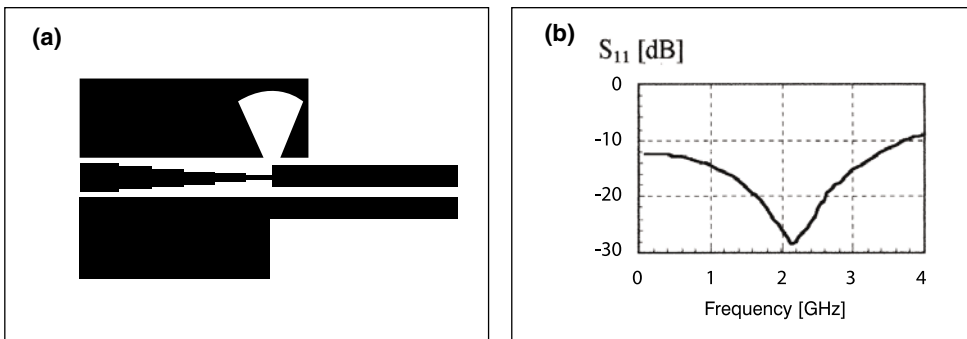
▲ Figure 2. (a) Diagram of the coplanar waveguide (CPW) to coplanar strip (CPS) balun. (b) Simulated reflection coefficient S_{11}-parameter for one balun with the CPS terminated by an ideal 80 ohm resistor.

quency increases, the axial ratio decreases and the polarization becomes elliptical. For frequencies at which the arm lengths of the spiral antenna are greater than one wavelength, or slightly less, the polarization is circular and the input impedance remains almost constant as frequency varies [2, 9]. The spiral antenna is designed to meet conditions where circular polarization is required; thus. the minimum frequency is where the electrical length of the arm is one wavelength. For the antenna discussed here, the arm length is 0.52 m, which results in a resonant frequency of 0.58 GHz. This resonant frequency is likely lowered due to the dielectric-loaded substrate.

Balun configuration

The logarithmic spiral shown in Figure 1 is a balanced antenna and requires a balun to transform the unbalanced coplanar waveguide (CPW) feed line to a balanced coplanar strip (CPS) feed line for the logarithmic spiral antenna. In this article, the transition from CPW to CPS is accomplished by using a wideband balun [12]. This balun is a modified version of that in [11] and has also been used in [3] and [13].

The balun shown in Figure 2 includes a four section Chebyshev impedance transformer with a reflection coefficient of $\Gamma_m = 0.05$, which was designed to trans-

form the impedance from 50 to 80 ohms [12]. The input impedance of the spiral antenna is found to be approximately 80 ohms. The wideband transition from CPW to CPS is accomplished by using a slotted radial patch. The patch represents a very wideband open circuit, which forces the field to be primarily between the two conductors of the coplanar strip feed line. Two bond wires (not shown in the figure) near the discontinuity plane ensure that the potential on the two ground planes is equal [13]. The balun structure was fabricated on a small 16×43 mm RT/Duroid substrate with a thickness of 0.785 mm and a relative dielectric constant (ε_r) of 10.2.

Simulations on the balun structure shown in Figure 2(a) with IE3D are performed by substituting the antenna with an ideal 80-watt resistor. The results show that in the frequency range from 0.1 to 3.85 GHz the simulated reflection coefficient, i.e., the S_{11}-parameter, is better than –10 dB, as shown in Figure 2(b).

A more detailed description of the performance of the balun can be found in [13].

Numerical and experimental results

When the electrical size of the structure becomes too large, the benefits of using the IE3D are reduced. For example, simulations on the entire spiral antenna structure are not possible within a reasonable amount of time because of the limited computer capacity. To solve this problem, the spiral antenna is broken up into smaller parts, as illustrated by the different colors in Figure 3. The electrical size of the spiral increases as the frequency increases. The entire structure is first simulated in the frequency range from 0.1 to 1.4 GHz. Then, the fractions of the two arms, which correspond to the blue parts shown in Figure 1, are removed. Consequently, simulations are performed in a frequency range that is shifted upwards, that is, the influence of the blue parts are neglected. However, inaccuracies can occur when the currents on the arms that are removed are not negligible. A less effective way to solve this problem is to use a faster computer.

The balun structure was fabricated and connected to the fabricated prototype of the spiral antenna to verify
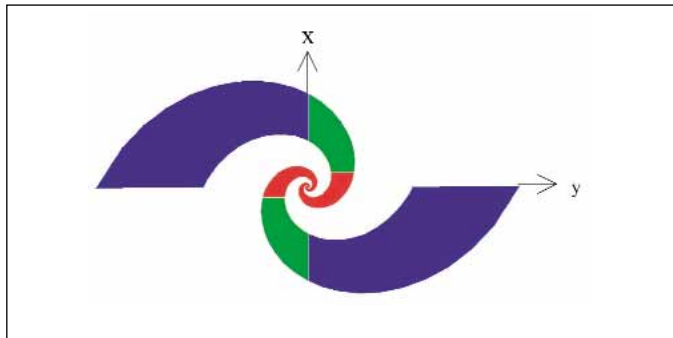
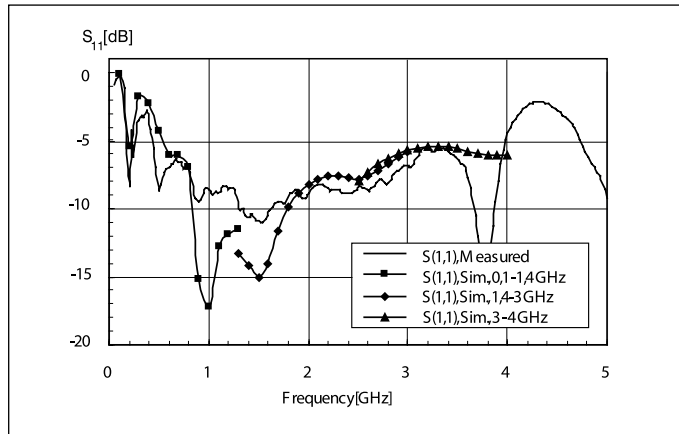▲ **Figure 3. The spiral is broken up into smaller parts to reduce the simulation time.**
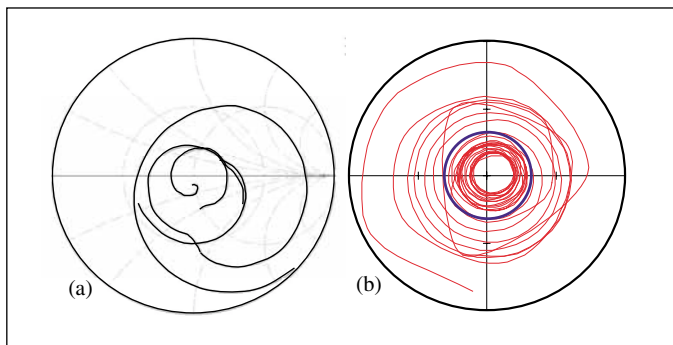
▲ **Figure 5. Simulated (a) and measured (b) impedances for the CPW-fed spiral antenna. The measured results show several loops in the Smith chart that are caused by a 0.4 m RG316U coaxial cable connected to the CPW on the balun. The circle shown in (b) indicates that every point inside the circle has an impedance match better than –10 dB.**

▲ **Figure 4. Measured and simulated S_{11}-parameter for the CPW-fed spiral antenna on FR-4 substrate material.**

the performance. The reflection coefficient of the spiral antenna, S_{11}, including the CPW- to CPS-feed network is determined using an HP8720D network analyzer. The experimental results are shown in Figure 4 for the CPW-fed spiral antenna.

The measured and simulated results are shown in Figure 4. The best agreement is achieved with large reflection coefficients, i.e., for $S_{11} > –10$ dB. The measured bandwidth for a reflection coefficient better than –6 dB is just slightly higher than the simulated. The measured bandwidth is from 0.45 to 3.1 GHz, and the simulated bandwidth is from 0.6 to 2.9 GHz. At a frequency of 3.8 GHz, the measured impedance matching is much better than the simulated. This may be due to parasitic coupling between the antenna and the balun.

The simulated input impedance of the spiral antenna is 80 ohms. The measured and the simulated impedances for the spiral antenna including the CPW- to CPS-feed network is found to be matched to 50 ohms, as shown in the Smith charts shown in Figure 5. Because of the electrical length of the 0.4 m RG316U coaxial cable, the measured impedance is mapped into the

Smith chart as a spiral located around the center of the Smith chart. This indicates that the spiral antenna, including the feed structure, is close to being matched to 50 ohms.

Simulations of two identical spiral antennas placed on two different substrates are made. The substrates used are FR-4 with a relative permittivity of 4.4 and ROHACELL with a relative permittivity of 1.06. The simulated results state that the input impedance for the spiral placed on the FR-4 is 80 ohms, whereas the impedance for the spiral antenna placed on ROHACELL is 130 ohms. This indicates that increasing the relative permittivity on the substrate could lower the input impedance. The result is in agreement with a recently published spiral antenna with an input impedance of 61 ohms. This antenna was placed on a substrate with a relative permittivity of 10.8 [11].
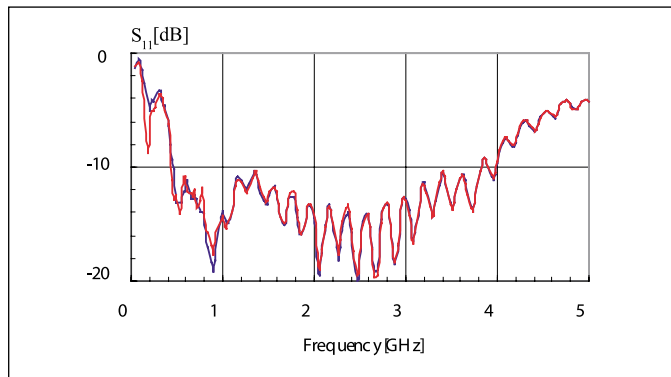
Cavity-backed spiral antenna

The planar logarithmic spiral antenna radiates in two broad lobes whose directions are perpendicular to the plane of the antenna. However, a unidirectional pattern is preferred in order to detect reflections from one direction only; thus, a cavity is needed. An absorbing material and polystyrene foam with thicknesses of 130 mm and 40 mm, respectively, fill up the back of the constructed cavity [14]. Figure 6 shows an illustration of the cavity. The overall size of the cavity is $610 \times 290 \times 180$ mm.

Figure 7 shows the experimental results for the CPW-fed spiral antenna backed with a cavity. The measured bandwidth for a reflection coefficient better than –10 dB is from 0.4 to 3.8 GHz. The main reason for the extended bandwidth as compared to the S-parameters shown in Figure 4 is the balun. In this case, the balun approach shown in Figure 2 is applied, whereas the balun used in the experiment in Figure 4 consists of a balun optimized for an approach other than the fabricated spiral antenna. The observed ripple on the measured reflection coef-
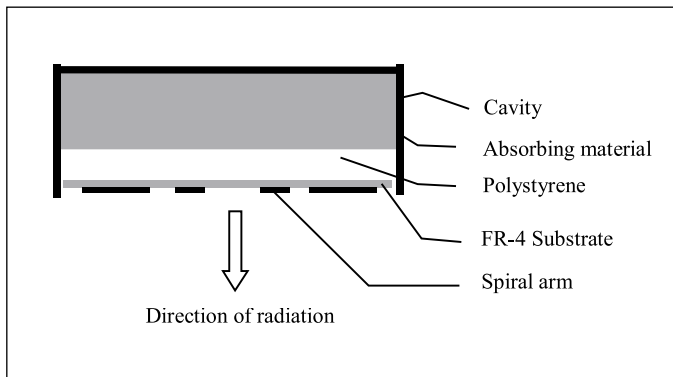
▲ **Figure 6. Cross section illustration of the cavity backed spiral antenna.**

▲ **Figure 7. Measured S_{11}-parameter for the spiral antenna with (red) and without (blue) a cavity.**
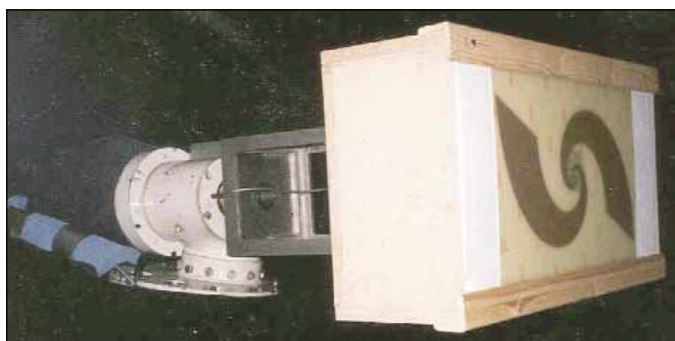
▲ **Figure 8. Picture of the cavity backed spiral antenna mounted in the anechoic chamber.**

ficient is likely to be caused by a mismatch with the 0.4 m RG316U flexible coaxial cable that is connected to the CPW on the balun.

Limitations on available computer capacity make it too time consuming to simulate the absorbing material using IE3D. In Figure 7, the measured S_{11}-parameter for the cavity backed spiral antenna can be compared to the measured S_{11}-parameter for the spiral antenna without a cavity. Little difference is observed in the S_{11}-parameter for the spiral antenna with or without a cavity. This result indicates that the radiation in the main direction remains virtually unchanged in the presence of the cavity.

Far-field radiation patterns

Anechoic chamber measurements in the Sperical Nearfield Antenna Test Facility (SNATF) at the Technical University of Denmark (DTU) are made in order to measure the far-field radiation pattern and the polarization. A picture of the spiral antenna situated in the anechoic chamber is shown in Figure 8.

Two θ-cuts, measured at 0.8 GHz and 1.5 GHz, are shown in Figure 9. Relevant far-field criterion is fulfilled, so the measured data can be used directly, without a near-field-to-far-field transformation.

From a theoretical point of view, the spiral antenna has a broad bi-directional radiation pattern with the two maxima perpendicular to the plane on which the spiral antenna is located, the *xy*-plane, as shown in Figure 1. Simulations performed without any absorbing material have verified this pattern.

The measured radiation patterns shown in Figure 9 display a minor asymmetry of the main beam at both frequencies. This asymmetry is caused by the asymmetry in the CPS of the balun. At 0.8 GHz, the front to back ratio is 10 dB. This ratio is increased to 15 dB at 1.5 GHz because the attenuation in the absorbing material increases with the frequency.

At a frequency of 0.8 GHz, the simulated directivity is 5.6 dB, which is only 0.2 dB below the measured directivity estimated from the measured HPBW. In the frequency range between 0.5 and 2.6 GHz, the directivity is estimated to be in the range between 2.7 and 6.6 dB, using the measured HPBW.

The antenna is designed to meet conditions where circular polarization is required. A commonly used criterion states that the axial ratio should be less than 6 dB [9]. The axial ratio shown in Figure 10 indicates that the spiral antenna is circular polarized in the $\theta = 0$ degrees direction at frequencies between 0.5 and 2.6 GHz. For frequencies above 2.6 GHz, the axial ratio is not measured, but circular polarization is expected up to a certain frequency point where the size of the feed region, i.e., the center of the spiral, becomes small compared to the balun structure. This frequency limit is expected to be near the frequency limit for acceptable S_{11}-parameter, which is around 3.8 GHz (Figure 7). Above 3.8 GHz, it is likely that the polarization ellipse becomes even more elliptic.

The polarization ellipse is somewhat elliptical at a frequency of 2.6 GHz, as shown in Figure 10(b). This phenomenon can also be observed in Figure 9 as a difference in the amplitude in the $\theta = 0$ degrees direction for the measured θ-cuts.

For a frequency independent antenna, the radiation

(a) Mag. [dB]

(b) Mag. [dB]
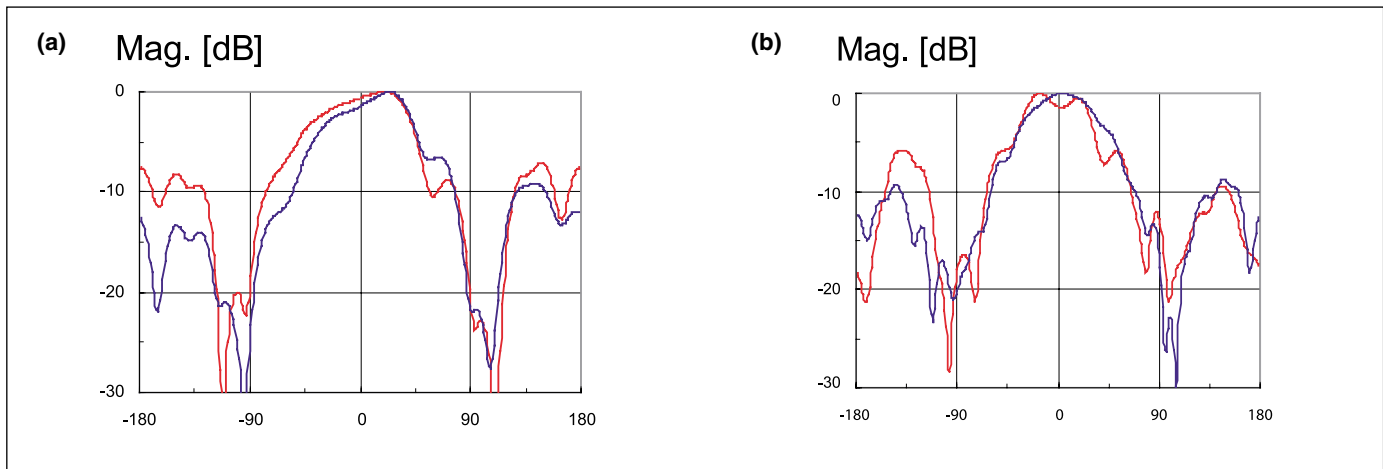
▲ **Figure 9. Measured θ-cuts for $\phi = 0$ degrees (red) and for $\phi = 90$ degrees (blue). Positive values of θ' correspond to $\phi = \phi_0$, and $\theta = \theta'$ and negative value of θ' corresponds to $\phi = \phi_0 + 180$ degrees, $\theta = -\theta'$, with respect to the polar orientation of the spiral antenna at frequencies of (a) 0.8 GHz and (b) 1.5 GHz.**

(a) AR [dB]

(b) y
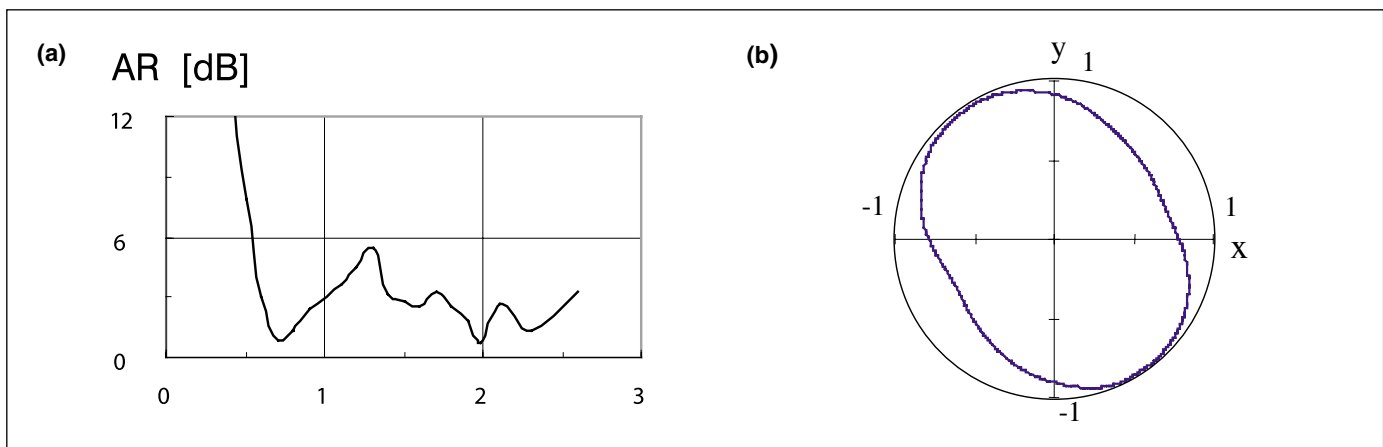
▲ **Figure 10. (a) Measured axial ratio vs. frequency and (b) measured polarization ellipse at a fequency of 2.6 GHz.**

**(a)** $\phi=0$ **(b)**

$\phi=90$
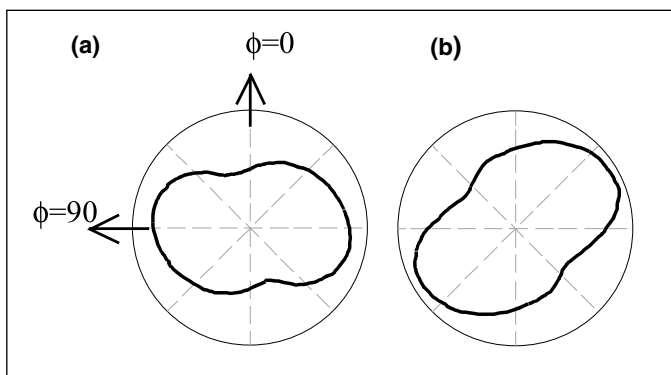
▲ **Figure 11. Simulated radiation pattern at a ϕ cut for $\theta = 60$ degrees obtained at (a) 0.8 GHz and (b) 1.3 GHz.**

should be unchanged at all frequencies, except for a rotation around the polar axis [2]. The results from the simulations of the radiation at a ϕ cut at two frequencies

are shown in Figure 11. The radiation pattern is rotated around the polar axis. The design equations for the spiral antenna state that the relationship for the angle of the rotation, $\Delta\phi$, as a function of the initial upper frequency and the lower frequency, is given by $\Delta\phi=a^{-1}ln(f_{upper}/f_{lower})$ [2], where a is the growth rate. When using this equation, the theoretical angle of rotation between 1.3 GHz and 0.8 GHz is 55 degrees, which is in good agreement with the simulated angle obtained from Figure 11. The simulated angle of rotation is 52 degrees. Therefore, it is very likely that the spiral antenna radiates from an active region that is dependent on the frequency of operation.

Note that for a theoretical model of the structure of the spiral antenna there is no particular feeding point, and the active region should begin at a frequency dependent point on the antenna. The present result seems to contradict the theoretical model. The viewpoint of the theoretical model is in accordance with the
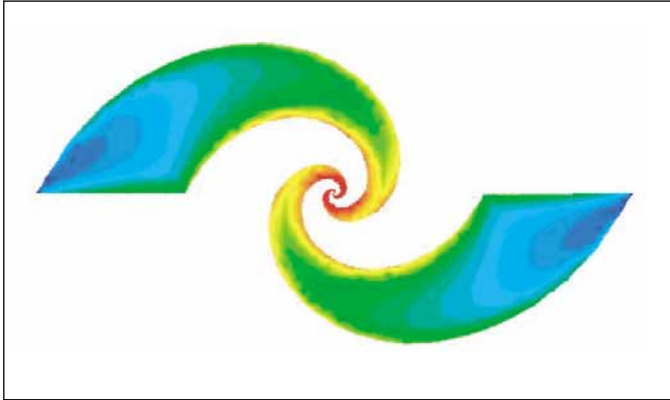
▲ **Figure 12. Illustration of the 1.5 turn coplanar strip fed logarithmic spiral antenna. Simulation of the average current distribution on the metallic surface of the spiral antenna, by using IE3D. Red illustrates the highest current intensity and blue illustrates the lowest current intensity, both at 0.5 GHz.**

rotation of the radiation pattern. The reason may be that the region near the feed point contributes only a little. Note that the measured rotation is 52 degrees and the theoretical is 55 degrees between 1.3 GHz and 0.8 GHz. Since the region near the feed point contributes, the rotation is less than expected from theory. This aspect is examined [15]. There, Thaysen, et al, discuss the relation between the angle of rotation of the radiation pattern and the position of the current active region on the spiral antenna.

If the antenna is constructed so that the initial radius r_0 is only a fraction of a wavelength and is excited from a transmission line connected at the small end, a current wave travels out from the feed point along the arms. As the energy radiates, the amplitude of the current decreases. This effect can be observed in Figure 12, where the average current density is shown for a frequency of 0.5 GHz. This current distribution is calculated using IE3D. The result shows that the average current density is located symmetrically on the two spiral arms with the highest current density at the feed point and at the edges. Also, a slight decrease in current density as a function of the distance from the feed points is observed and is indicated by a shift in color from red to blue.

Conclusion

This article discussed the design and model of a spiral antenna for the FR-4 substrate, and a balun for the RT/Duroid substrate. The electromagnetic simulation program IE3D has been used to simulate the performance of the spiral antenna.

Good agreement was shown between the numerical results and the measured results obtained using a network analyzer in the frequency range from 300 kHz to 5 GHz. The measured reflection coefficient for the fabri-

cated spiral antenna shows a slightly better performance than the simulated results, which is most likely due to computer capacity limitations. The measured reflection coefficient is better than –10 dB, over a 9 to 1 bandwidth from 0.4 to 3.8 GHz.

An inverse proportionality between the input impedance and the relative permittivity of the substrate was found. The simulations and the measurements of the spiral antenna show that the radiation pattern and the input impedance are essentially constant over a bandwidth larger than 9 to 1.

Measurements in an anechoic chamber from 0.8 GHz to 2.6 GHz are made showing an axial ratio of less than 3.3 dB and a directivity in the range between 2.7 and 6.6 dB. At a frequency of 0.8 GHz, the simulated directivity is 5.6 dB, only 0.2 dB below the measured directivity.

From the simulated ϕ cuts at two different frequencies, it is shown that the radiation pattern rotates around the polar axis as a function of the frequency.

The simulated current distribution on the metallic surface of the spiral antenna shows that the average current distribution decreases as a function of the distance from the feeding point.

The constructed uniplanar spiral antenna and the balun are well-suited for use in a stepped frequency ground penetrating radar for humanitarian demining because of the spiral's wide bandwidth, circular polarization, relatively small size, inexpensive cost and uniplanar design. ■

References

1. P.E. Mayes, "Frequency-independent Antennas and Broadband Derivatives Thereof," *Proceedings of the IEEE*, Vol. 80, 1982: 103–112.

2. J.D. Dyson, "The Equiangular Spiral Antenna," *IRE Transactions on Antennas and Propagation,* 1959: 181–187.

3. J. Thaysen, et al, "Numerical and Experimental Investigation of a Coplanar Waveguide-Fed Spiral Antenna," *IEEE 24th QMW Antenna Symposium, 2000*: 13–16.

4. J. Thaysen, et al, "Ultra Wideband Coplanar Waveguide-Fed Spiral Antenna for Humanitarian Demining," *30th European Microwave Conference*, CNIT, La Defense, Paris, (October 2–5, 2000): 371–375.

5. D.M. Pozar, *Microwave Engineering, 2nd Ed.*, New York: John Wiley & Sons, 1998.

6. "IE3D User's Manual, Release 6," Zeland Software, Inc., Fremont, CA, 1999.

7. J. Thaysen, "Broadband Antennas," Department of Applied Electronics, Technical University of Denmark, July 1999.

8. J.D. Dyson, "The Unidirectional Equiangular Spiral Antenna," *IRE Transactions on Antennas and Propagation*, 1959: 329–334.

9. J. Thaysen, "Logarithmic Spiral Antenna and Feed Network for Application to Humanitarian Demining," Department of Applied Electronics and Department of Electromagnetic Systems, Technical University of Denmark, Master Thesis in Danish, March 2000.

10. K. Tilley, et al, "Coplanar Waveguide Fed Coplanar Strip Dipole Antenna," *Electronics Letters*, Vol. 30, 1994: 176–177.

11. M-Y. Li, et al, "Broadband Coplanar Waveguide-Coplanar Strip-fed Spiral Antenna," *Electronics Letters*, Vol. 31, 1995: 4–5.

12. J. Thaysen, et al, "Characterization and Optimization of a Coplanar Waveguide Fed Logarithmic Spiral Antenna," *IEEE AP-S Conference on Antennas and Propagation for Wireless Communication*, Waltham, MA, 2000: 25–28.

13. J. Thaysen, et al, "A Wideband Balun — How Does it Work?," *Applied Microwave and Wireless*, Vol. 12, No. 10, October 2000: 40–50.

14. R.G. Corzine, and J.A. Mosko, *Four-Arm Spiral Antennas*, Artech House, 1990.

15. J. Thaysen, et al, "The Radiation Pattern of a Logarithmic Spiral Antenna," Accepted for presentation at the *2001 URSI International Symposium on Electromagnetic Theory*, Victoria, British Columbia, Canada, (May 2001): 4.

Author information

Jesper Thaysen received his M.Sc.E.E. degree from the Technical University of Denmark, Lyngby, in 2000. He currently works as an electronic engineer at the Technical University of Denmark. He can be reached via e-mail at jt@iae.dtu.dk.

Kaj B. Jakobsen received his M.Sc.E.E. degree from the Technical University of Denmark, Lyngby, in 1986, and his Ph.D. from University of Dayton, Ohio, in 1989. Currently an associate professor at the Technical University of Denmark, he can be reached via e-mail at kbj@iae.dtu.dk.

Jørgen Appel-Hansen received his M.Sc.E.E. degree and Ph.D. from the Technical University of Denmark, Lyngby, in 1962 and 1966, respectively. Currently an associate professor at the Technical University of Denmark, he can be reached via email at jah@emi.dtu.dk.

All three authors can also be reached at Department of Electromagnetic Systems (EMI), Bldg. 348, Technical University of Denmark, DK-2800 Kgs. Lyngby, Denmark; Tel: +45 4588 1444; Fax: +45 4593 1634.